

DISTRIBUTED GENERATION SYSTEM USING HYBRID RENEWABLE ENERGY SOURCES

A PROJECT REPORT

Submitted by

HRITHIK VEL B (913119105022)

JEY VISHNU V.BA (913119105028)

VIJAY KRISHNA T.K.B (913119105304)

in partial fulfillment for the award of the degree

of

BACHELOR OF ENGINEERING

IN

ELECTRICAL AND ELECTRONICS ENGINEERING

VELAMMAL COLLEGE OF ENGINEERING AND TECHNOLOGY

(Autonomous)

MADURAI-625009

ANNA UNIVERSITY:: CHENNAI 600 025

MAY 2023

BONAFIDE CERTIFICATE

Certified that this project “**DISTRIBUTED GENERATION SYSTEM USING HYBRID RENEWABLE ENERGY SOURCES**” in the bonafide work of HRITHIK VEL B (913119105022), JEY VISHNU V.BA(913119105028) and VIJAY KRISHNA T.K.B (913119105304) who carried out the project under my supervision.

SIGNATURE

Dr.R.NARMATHA BANU,M.E.,Ph.D.,

PROFESSOR

HEAD OF THE DEPARTMENT

Electrical and Electronics Engineering

Velammal College of Engineering and
and Technology

Madurai – 625 009

SIGNATURE

Dr.S.CHELLAM M.E,PH.D.,

ASSISTANT PROFESSOR

SUPERVISOR

Electrical and Electronics Engineering

Velammal College of Engineering
and Technology

Madurai – 625 009

Certified that the candidate was examined on the Viva-Voice Examination held at Velammal College of Engineering and Technology, Madurai on _____ .

INTERNAL EXAMINER

EXTERNAL EXAMINER

ACKNOWLEDGEMENT

First of all we thank the Almighty for strengthening us throughout the project and helping us to complete it successfully.

We find immense pleasure to convey our sincere thanks to our honorable Senior Principal **Dr.N.SURESH KUMAR,M.E.,Ph.D.,** and Principal **Dr.P.ALLI,B.E.,M.S.,Ph.D.,** for providing necessary facilities in carrying out our project work in our campus.

We would like to express our hearty thanks to our Dean of the Department **Dr.A.SHUNMUGALATHA,M.E.,Ph.D.,** and Head of the Department **Dr.R.NARMATHA BANU,M.E.,Ph.D.,** for constant encouragement.

We take this opportunity to express our sincere and heartfelt thanks to our guide, **Dr.S.CHELLAM,M.E.,PH.D.,** for her patient guidance, timely suggestion, technical and moral support and the immense part of his dedication in completing the project work successfully.

We express our special thanks to all teaching faculty of our department, the non-teaching faculty and our friends who assisted us, by their support and encouragement.

We also express our special thanks to our Parents who have sacrificed greatly in our education and welfare. We thank all those who have helped directly and indirectly in doing this project and bringing out this successful report.

ABSTRACT

Micro-grids are small-scale power grids that integrate clean and/or conventional generation systems into a unified power system for robust, reliable, resilient, and sustainable load support. They provide an attractive ability to sense critical changes in the utility grid to facilitate an autonomous control action to disconnect from the utility grid into the island mode. A real-time integrated model of a micro-grid to simulate its electrical energy infrastructure. The design includes two PV arrays, a fuel cell, and a diesel generator that support building loads when islanded from the utility grid.

In contrary to the conventional microgrid configurations this project proposes a new topology of a hybrid distributed generator based on photovoltaic and wind-driven permanent magnet synchronous generator, which are together connected to the grid with the help of only a single boost converter followed by an inverter. Thus, compared to earlier schemes, the proposed scheme has fewer power converters.

Two separate controllers are also proposed for the new hybrid scheme to separately trigger the DC-DC converter and the inverter for tracking the maximum power from both the sources. The integrated operations of both the proposed controllers for different conditions are demonstrated through simulation and experimentation. Steady-state performance of the system is also presented to demonstrate the successful operation of the new hybrid system. Comparison of experimental and simulation results are given to validate the simulation model.

TABLE OF CONTENTS

S.No	Title	Page No
	ACKNOWLEDGEMENT	i
	ABSTRACT	ii
	LIST OF FIGURES	v
	LIST OF TABLES	vii
	LIST OF ABBREVIATIONS	viii
1	CHAPTER 1: INTRODUCTION	1
	1.1 Microgrid System Description	6
2	CHAPTER 2: LITERATURE SURVEY	8
3	CHAPTER 3: EXISITING METHODLOGY	15
	3.1 Models Of Distributed Generation	15
	3.1.1 PV Array Model	17
	3.1.2 Fuel Cell Model	19
	3.1.3 Diesel Generator Model	22
	3.2 Inverter control and synchronization	24
4	CHAPTER 4: PROPOSED METHOD	26
	4.1 Introduction	26
	4.2 Proposed DG Scheme	27
	4.3 Maximum Power Point Tracking Algorithms	28
	4.4 Models Of The Proposed System	29
	4.5 Operation Of The Controllers	33
	4.6 Implementation Of The Controllers	36
5	CHAPTER 5: RESULT AND DISCUSSIONS	38
	5.1 Existing Method	38
	5.2 Proposed Method	39

	5.3 Comparison between Existing System and Proposed System	47
6	CHAPTER 6: CONCLUSIONS AND FUTURE SCOPE	48
	6.1 Conclusions	48
	6.2 Future Scope	49
	REFERENCES	52

LIST OF FIGURES

Fig No	Title	Page No
Fig 3.1	High-level block-diagram of the micro-grid	16
Fig 3.2	Non - ideal fuel cell model as a controlled voltage source taking into account various losses	16
Fig 3.3	Non-ideal PV array model as a controlled voltage sources	17
Fig 3.4	Diesel generator model	17
Fig 3.5	Perturbation and observation method	19
Fig 3.6	Diesel engine governor mode	22
Fig 3.7	Closed-loop control for three phase inverter	24
Fig 3.8	Synchronized source	24
Fig 4.1	Proposed DG system based on PMSG-PV sources	27
Fig 4.2	Per-phase steady state equivalent circuit of PMSG	29
Fig 4.3	d-axis equivalent of the system	32
Fig 4.4	q-axis equivalent of the system	32
Fig 5.1	Simulation model contain PV, dc-dc converter and utility grid	38
Fig 5.2	MATLAB simulation of the Grid Connected Hybrid Wind- Driven PMSG-PV System	39
Fig 5.3	MATLAB simulation of wind Model	40
Fig 5.4	MATLAB simulation of PV Model	41
Fig 5.5	PV panel properties	41
Fig 5.6	Characteristics of a single module	42
Fig 5.7	Changes in rectifier output voltage and duty cycle of boost converter	42
Fig 5.8	DC link voltage control	43

Fig 5.9	Inverter output voltage	44
Fig 5.10	Steady-state grid voltage and current waveforms	44
Fig 5.11	Harmonic analysis of grid voltage	45
Fig 5.12	Harmonic analysis of grid current	46

LIST OF TABLES

Table No	Title	Page No
Table 4.1	Functions of controllers under different conditions	35

LIST OF ABBREVIATIONS

VOC	Open Circuit Voltage of PV array (V)
VS	PMSG stator voltage (V)
Vb	VDC Boost converter output voltage (V)
VR	Rectifier output voltage (V)
Vpv	PV array terminal voltage (V)
Vm	Maximum power point voltage of PV array (V)
VGRID	Output voltage of the inverter (V)
vGd, vGq	d-axis and q-axis voltage of grid (V)
vd, vq	d-axis and q-axis voltage of inverter (V)
E Stator	EMF of PMSG (V)
ISC	Short circuit current of PV array (A)
IS	PMSG stator current (A)
IR	Rectifier output current (A)
Ib	Boost converter output current (A)
IDC	DC link current (A)
IGRID	Output current of the inverter (A)
Ipv	Current from PV array (A)
Id	Current through internal diode of PV array (A)
Im	PV array current at maximum power point (A)

CHAPTER 1

INTRODUCTION

With the rise of concerns regarding traditional power systems' vulnerability to physical attacks, cyber-attacks, or failures due to natural disasters or aging, trends in power systems research have turned toward the development of distributed micro-grids. Micro-grids are small-scale power grids that integrate clean and/or conventional generation systems into a unified power system for robust, reliable, resilient, and sustainable load support. They provide an attractive ability to sense critical changes in the utility grid to facilitate an autonomous control action to disconnect from the utility grid into the island mode. The ability of these microgrids to disconnect and reconnect to the utility grid creates transient properties that must be controlled in order to maintain stable and sustainable power.

When the micro-grid is grid-tied, it is common to have synchronous connection where all micro-grid voltages must be synchronized with the utility grid, and later operate at desired voltage and frequency in the island mode. Harmonics, synchronization, voltage sags, failure of rotating machinery, and many other anomalies could arise when voltage and frequency conditions are not met. Asynchronous interconnection and DC micro-grids are expected to be viable alternatives to mitigate the frequency and synchronization requirements. For existing and near-future micro-grids, the detailed simulation models, including high levels of clean energy penetration, must be established.

Throughout literature, modeling approaches to micro-grids have been very limited. One approach was through the development of inverter-based models. These assume that distributed generators output a DC voltage that gets synchronized to the utility grid through inverters even though some conventional sources with diesel and natural gas are AC. Others have modeled micro-grids with off-the-shelf libraries, e.g. Simulink in islanded mode but did not analyze various system integration and time scale requirements, e.g. several hours of simulation time that can take several days or weeks to process. Other literature has focused on microgrid control methods based on small signal models in state-space format where eigenvalues are utilized for control. Other approaches to modeling have tried studying the behavior of a micro-grid with electrical energy storage devices under utility grid disturbances and for lifetime analysis of the micro-grid in island mode.

Recently renewable energy sources are attractive options for providing power in places where a connection to the utility network is either impossible or unduly expensive. As electric distribution technology steps into next century, many trends are becoming noticeable that will change the requirements of energy delivery. The ever increasing energy consumption, soaring cost and exhaustible nature of fossil fuels, and the worsening global environment have created increased interest in green power generation systems.

Renewable sources have gained worldwide attention due to fast depletion of fossil fuels along with growing energy demand. DC power from photovoltaic panels (PV) or fuel cells has to be converted into ac using dc/dc boosters and dc/ac inverters in order to connect to an ac grid. Recently, DC micro grids are resurging due to the development and deployment of renewable dc

power sources and their inherent advantage for dc loads in commercial, industrial and residential applications.

Most literature focuses on modeling one or two aspects of the micro-grid, but no model exists that integrates the electrical energy infrastructure as loads, distributed generation, energy conversion (power electronics), control at component levels, system integration, and real-time simulation. The power system simulators, meanwhile, the investigation of grid-tied power electronics usually ignores generator models and their transient impact, but both levels of systems and their transients are considered and analyzed in the existing work to provide a more realistic model of a micro-grid. Note that the model presented here and which is formed by integrated several other models can be used as an example to apply a similar approach to this presented here for other micro-grids.

This existing work aims to develop detailed models of a real micro-grid's electrical energy infrastructure. This includes clean and conventional generation systems: two PV arrays, a fuel cell, a diesel generator, inverters and their interconnections. Each generation system has voltage control with inverter voltages synchronized using phase lock loops (PLLs). Once all models are implemented into a larger micro-grid model, case studies are simulated on a Simulink Real Time platform.

A microgrid installed with distributed generations (DGs) is a new type of power system. DGs, which include micro turbines, photovoltaics, wind cells, and fuel cells, are small generation units of less than 100 kW. At present, power systems are experiencing a rapid growth in the connection of DG units. Integrating DGs in a distribution system offers technical, environmental, and economic benefits. Moreover, such integration allows distribution utilities to improve system

performance by reducing power losses. Electric energy market reforms and developments in electronics and communication technology enable the advanced control of DGs.

The DC micro grid has been proposed to incorporate various distributed generators and ac sources have to be converted into dc before connected to a dc grid and dc/ac inverters are required for conventional ac loads. DC micro grid cannot completely eliminate losses occurring in multiple stage conversions, though losses occurring in dc/dc conversions are lesser than those occurring in dc/ac or ac/dc conversions. Multiple reverse conversions are required in an individual ac or dc grids may add additional loss to the system operation and will make current home and office appliances more complicated. Thus, a hybrid micro grid is more beneficial to reduce the processes of multiple reverse conversions in an individual ac or dc micro grid to facilitate the connection of variable renewable ac and dc sources and loads with the power system in order to minimize the conversion losses. Since the operational issues of hybrid grid is more complicated than those of an individual ac and dc micro grids. A micro grid comprises of low voltage distributed systems with distributed generations, storage devices, loads and interconnecting switches. The operation of micro grids provide advantages of higher flexibility, better power quality, controllability, efficiency of operation, and bidirectional power flow between the utility grid and the micro grid in the grid connected mode of operation.

DG units can be integrated and efficiently operated as a microgrid in grid-connected and islanded modes. A microgrid system can strategically be placed on any site in a power system for grid reinforcement, thereby deferring or eliminating the need for system upgrades and improving system integrity, reliability, and

efficiency of the existing power system. Therefore, many efforts have been exerted to control power electronic converters and thus allow the grid connection of microgrids in a distribution system. This technique is necessary to maximize the potential of DGs to enhance power quality and reliability and provide auxiliary services, such as active reserve, load following, interruptible loads, reactive reserve, and restoration. A microgrid operated in islanded mode is controlled by several inverters connected in parallel and sharing load to maintain voltage and frequency.

Among the various techniques applicable to parallel inverter control in islanded mode operation, voltage and frequency droop based methods are appropriate to fulfill the requirements for communications control. Active power acts on voltage, and reactive power acts on frequency. That is, the active power output is dependent on local voltage. PI controllers have simple control structures and maintenance.

However, the performance of these controllers degrades as the system operating conditions change. Fuzzy logic controllers are superior to conventional controllers because they can be easily adapted to different system structures, parameters, and operation points. In addition, they can be implemented in large-scale nonlinear systems. Thus, many researchers have attempted to combine conventional PI with fuzzy logic controllers to improve performance.

A hybrid ac/dc micro grid is proposed in this work to reduce processes of multiple reverse conversions in an individual ac or dc grid and to facilitate the connection of various renewable ac and dc sources and loads to power system. Since energy management, control, and operation of a hybrid grid

are more complicated than those of an individual ac or dc grid, different operating modes of a hybrid ac/dc grid have been investigated.

DG units can be integrated and efficiently operated as a microgrid in grid-connected and islanded modes. A microgrid system can strategically be placed on any site in a power system for grid reinforcement, thereby deferring or eliminating the need for system upgrades and improving system integrity, reliability, and efficiency of the existing power system. Therefore, many efforts have been exerted to control power electronic converters and thus allow the grid connection of microgrids in a distribution system. This technique is necessary to maximize the potential of DGs to enhance power quality and reliability and provide auxiliary services, such as active reserve, load following, interruptible loads, reactive reserve, and restoration

A microgrid operated in islanded mode is controlled by several inverters connected in parallel and sharing load to maintain voltage and frequency. Among the various techniques applicable to parallel inverter control in islanded mode operation, voltage and frequency droop based methods are appropriate to fulfill the requirements for communications control.

Active power acts on voltage, and reactive power acts on frequency. That is, the active power output is dependent on local voltage. PI controllers have simple control structures and maintenance. However, the performance of these controllers degrades as the system operating conditions change.

Fuzzy logic controllers are superior to conventional controllers because they can be easily adapted to different system structures, parameters, and operation points. In addition, they can be implemented in large-scale nonlinear systems.

Thus, many researchers have attempted to combine conventional PI with fuzzy logic controllers to improve performance.

1.1 Microgrid System Description

It illustrates a block diagram of the proposed microgrid system with VSI. As illustrated, this system consists of the control system and an inverter with filter that interfaces the DGs with the grid. The DGs generally used in a microgrid are photovoltaic, fuel cell, and micro turbine generators. The configuration and utilization of a set of DGs usually depend on customer needs and load criticality. The DC power sources can either be directly interfaced to the AC system through an inverter or be first set to an inverter compatible DC voltage level using a DC–DC converter and then converted into three phases using an inverter. AC power sources (e.g., microturbines) that produce power at high frequencies are first rectified and then converted to three-phase.

The loads within a microgrid can either be electrical and/or thermal in nature. They can be further classified into critical and non-critical loads. During islanding, load shedding of non-critical loads can be performed to maintain the power balance and hence stability of the microgrid system. Therefore, the critical loads can be continued to operate in a normal manner through load shedding.

The control system consists of several subsystems, including voltage and current control functions, grid synchronization function, and a pulse-width modulation (PWM) generator.

CHAPTER 2

LITERATURE SURVEY

Lasseter et al. (2019) has discussed as the scale of power systems gradually expands, large-scale blackouts occasionally happen, exposing the reliability and security issues of the power system. The construction and production mode of the power system produce a serious energy crisis and environmental problems. In this context, the microgrid has received much attention because of its reliability and high efficiency

Katiraeiet al. (2019) has discussedMicrogrids provide an effective technical means for the application of renewable energy. Since the access of many distributed generators (DGs) depends on inverters, the sources in microgrids are more flexible and controlled compared with conventional generators.

Hatziargyriouet al. (2018) has discussed that microgrids can operate in parallel to a grid and can work as an autonomous island by the rapid and robust control of power electronic devices. This allows microgrids to be used based on the operation condition of the distribution network or the economic requirements .

Chung et al. (2018) has discussed that the features of the microgrid can improve the security and reliability of the power supply, but it also produces many problems. The problem of transient dynamics is fundamentally important because it concerns the protection configuration, control strategy formulation, and transient stability assessment of the whole power system. However, studies on microgrids

have mainly concentrated on the system structure and control mode because the attention has been mainly on the realization of the microgrid.

Sortomme et al. (2017) has discussed that studies on the transient dynamics of microgrids are few, and most of them are directed at macroscopic simulation analyses.

van der Schaft et al. (2017) has discussed that the standard way to analyze the dynamics of a power system is to model the physical system mathematically. Various features of power system models have been established based on decades of experience. Thus, standard models of synchronous generator of various orders that capture particular classes of problems exist. However, related studies on microgrids are still few.

Sao, C. K et al. (2016) has discussed that the use of a recently proposed dynamic model [11] needs considerations on certain prerequisites, including inverter type, switching frequency, and bandwidth, because it assumes that the DGs are ideal voltage sources.

Barklund et al. (2016) has discussed that another proposed microgrid model [12–14] captures the detail of the control loops of the inverter and contains a full dynamic model of the network. However, its emphasis is on the problem of state stability and small-signal dynamics of microgrid to assess the influence of controller. The dynamic equivalent method used to adopt port-based network modeling decomposes the overall system into subsystems interconnected with each other through pairs of variables.

Hao, J et al. (2015) has discussed network-reduction models represented by a set of ordinary differential equations are major methods. In these models, all loads are

converted to constant admittance, and the network is reduced to generator internal buses. These equivalents have caused many problems .

Chen, Weiqiang et al (2015) proposed a real-time integrated model of a micro-grid to simulate its electrical energy infrastructure is presented in [16]. This infrastructure includes two PV arrays, a fuel cell, and a diesel generator that support building loads when islanded from the utility grid. [16] reviews existing models, which are usually available either as 1) low-level dynamic models, along with power electronics for specific components, e.g. PV system or fuel cell, or 2) high-level such as with conventional power systems where power electronics are ignored due to their faster dynamics. The proposed modeling strategy for sustainable power generation is emphasized for both grid-connected and islanding modes and combines slow and fast dynamics where both a micro-grid and related power electronics dynamics are simulated to show how a high-fidelity model can be used in a dynamic micro-grid environment. A synchronized regulator for islanded mode is presented. The PV arrays and fuel cell are assumed to be always available and variable irradiance conditions (e.g. nighttime) and the change of hydrogen and oxygen densities of fuel cell are shown in [16]. The diesel generator is used for black start or when the utility grid voltage or frequency drop below a threshold during which potential grid collapse could occur and the micro-grid goes into the island mode. The micro-grid model is simulated using a real-time simulator so that longer case studies and scenarios can be studied without ignoring fast dynamics.

Theubou et al.(2015) proposed a model in order to reduce the carbon gas emissions, wind energy conversion systems are currently more and more connected to actual diesel power plants to provide electricity to small remote communities where the power grids are not available. As for classical power systems, the

stability analysis, prediction, identification, control and diagnostic of hybrid wind-diesel small grids need accurate modelling of its main components. The state space representation is known as the more suitable system representation for simulation, identification/diagnostic and stability studies purposes. In [17] a linear state modelling of a diesel generator is proposed. The global diesel generator model obtained from the superposition principle of its components is applied for stability analysis using the eigenvalues calculation.

Xiong et al (2014) proposed that microgrids can provide a more reliable power supply and can enable the interconnection of renewable energy. The microgrid has been recognized as one of the most important directions of power systems. The transient characteristics of the microgrid are very important for the planning and operation of the whole power system. However, its mechanism still needs further exploration because the circuit structure, control feature, and even the operation mode of the microgrid are quite different from those of the traditional power system. In this article, a dynamic model is proposed for a microgrid according to the difference in transient processes between the microgrid and the traditional grid. The model is expressed as a differential-algebraic equation system, so the structure of the microgrid and the physical meaning of original variables are preserved. The focal point in [18] is the fast control function of the inverter and the strong coupling between inverter and grid.

Brissette et al(2014) presents a simulation platform for the modeling and study of microgrid (MG) power systems. Using MathWorks Simulink modeling software, the platform provides a library of tools for designing and simulating the behavior of an MG on time scales from seconds to days. The library includes a collection of power system and power electronics components (sources, loads, switches, etc.) that may be arbitrarily configured.

Pawelek et al (2014) proposed that also facilitates the study of energy management systems (EMS), which optimize the behavior of certain controllable sources and loads according to programmed algorithms. User-generated EMS routines can be integrated into an MG model.

In [20], the application of energy storage for enhancing distributed energy sources penetration and contributing to better quality of energy delivery to customers was investigated. A simulation method was used to study the effectiveness of complex control algorithms of energy storage system enabling load leveling and simultaneous voltage stabilization effect in grid-connected microsystem.

Torreset al (2014) presents the modeling, simulation and real-time implementation of a laboratory-scale diesel generator emulator. The core of the digital implementation is a development kit based on the digital signal processor TMS320F2812, where the mathematical models of the controllers, diesel prime mover, coupling shaft and synchronous generator are computed in real-time. The interface with the load is a voltage source inverter. The capacitor voltages of the output filter are controlled to emulate the terminal voltages of the generator.

Yancheng et al (2014) proposed that dealing with the interface design and software development for proton exchange membrane (PEM) fuel cell modeling based on Matlab/Simulink environment. Three models used in the software, steady-state mode, dynamic model and thermodynamic model, are described first. These models are then implemented through the graphic user interface (GUI) programming by Simulink, and the simulation results are visualized. There are voltage overshoots/ undershoots appearing in the results, which is come from the

combination of electrical dynamic model and thermodynamic model. For the interface design and software development, a GUI file(*.fig) is designed in Matlab interactively, a main program (*.m) is coded using Matlab language, and a Simulink model (*.mdl) is designed based on the fuel cell model in the work. The Matlab main program calls Matlab GUI file and Simulink diagram to complete the fuel cell simulation. The software are applied to PEM fuel cell and solid oxide fuel cell (SOFC) successfully.

Youniset al (2014) presents a fuel cell model supplying three-phase DC/AC inverter. The fuel cell output voltage is proportional to the change of the air (oxidant) pressure, the hydrogen (fuel) pressure and the current withdrawn from the fuel cell. Three-phase DC/AC inverter used to supply the AC load. Symmetric space vector pulse width modulation used to drive the three-phase inverter so that minimum harmonic distortion on the load side voltage and current Simulation results provided to validate the design.

Katiraei et al (2013) presented that addresses real and reactive power management strategies of electronically interfaced distributed generation (DG) units in the context of a multiple-DG microgrid system. The emphasis is primarily on electronically interfaced DG (EI-DG) units. DG controls and power management strategies are based on locally measured signals without communications. Based on the reactive power controls adopted, three power management strategies are identified and investigated. These strategies are based on 1) voltage-droop characteristic, 2) voltage regulation, and 3) load reactive power compensation. The real power of each DG unit is controlled based on a frequency-droop characteristic and a complimentary frequency restoration strategy. A systematic approach to develop a small-signal dynamic model of a multiple-DG microgrid, including real and reactive power management strategies, is also

presented. The microgrid eigen structure, based on the developed model, is used to 1) investigate the microgrid dynamic behavior, 2) select control parameters of DG units, and 3) incorporate power management strategies in the DG controllers. The model is also used to investigate sensitivity of the design to changes of parameters and operating point and to optimize performance of the microgrid system.

Hoke et al (2012) has presents a method for minimizing the cost of electric vehicle (EV) charging given variable electricity costs while also accounting for estimated costs of battery degradation using a simplified lithium-ion battery lifetime model. The simple battery lifetime model, also developed and presented here, estimates both energy capacity fade and power fade due to temperature, state of charge profile, and daily depth of discharge. This model has been validated by comparison with a detailed model, which in turn has been validated through comparison to experimental data. The simple model runs quickly in a MATLAB script, allowing for iterative numerical minimization of charge cost.

CHAPTER 3

EXISTING METHOD

This work aims to develop detailed models of a real micro-grid's electrical energy infrastructure. This includes clean and conventional generation systems: two PV arrays, a fuel cell, a diesel generator, inverters and their interconnections. Each generation system has voltage control with inverter voltages synchronized using phase lock loops (PLLs). Once all models are implemented into a larger micro-grid model, case studies are simulated on a Simulink Real Time platform where the simulated system is shown in Fig. 3.1. Fig. 3.2 shows a higher-level block diagram of the same system. Note that R-L loads shown in orange in Fig. 3.1 were extracted as average values from real dynamic building loads.

3.1 Models of distributed generation

Each distributed generator is grid-tied through power electronics where a DC/DC stage regulates individual DC busses and a DC/AC stage inverts to synchronize with the grid or other sources, except for diesel generators. The PV arrays' voltage levels allow for the use of a buck converter to regulate higher voltage from the PV model to lower voltage at the DC bus. Local sources support building loads in grid-tied and island modes. Figs 3.2-3.4 show generation model block diagrams. Note that PCC is the point of common coupling.

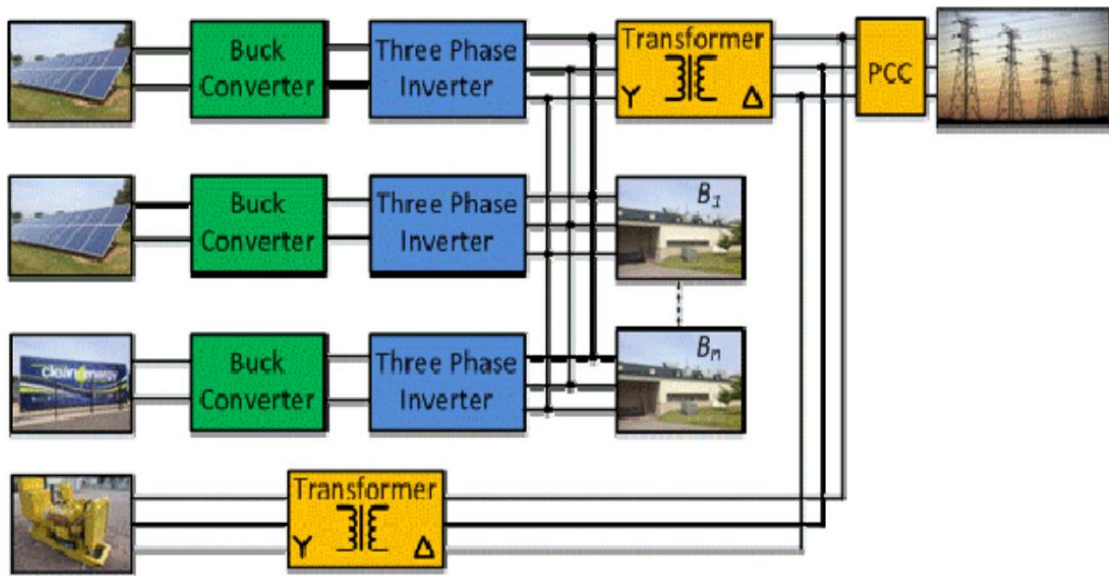


Fig. 3.1 High-level block-diagram of the micro-grid

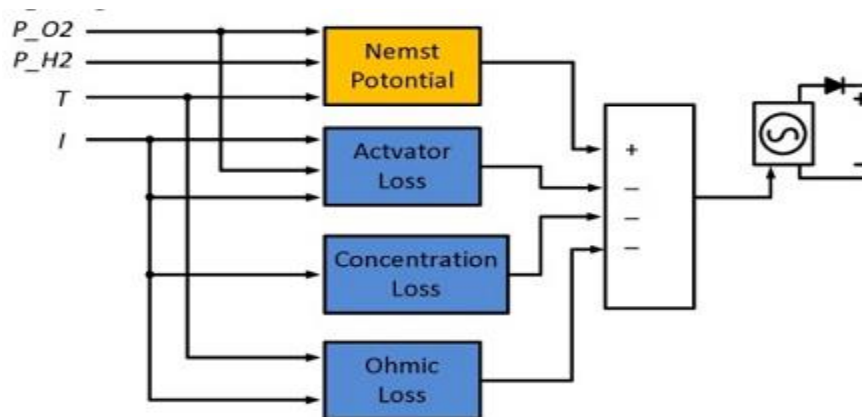


Fig. 3.2 Non - ideal fuel cell model as a controlled voltage source taking into account various losses

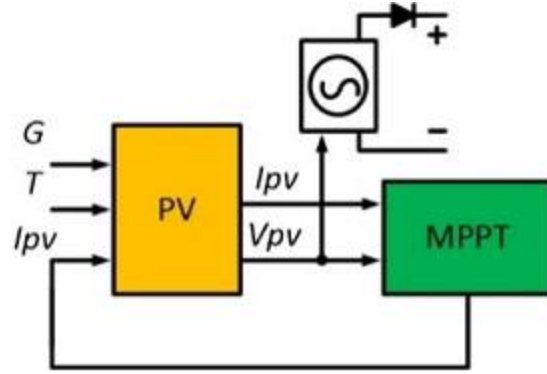


Fig. 3.3 Non-ideal PV array model as a controlled voltage source

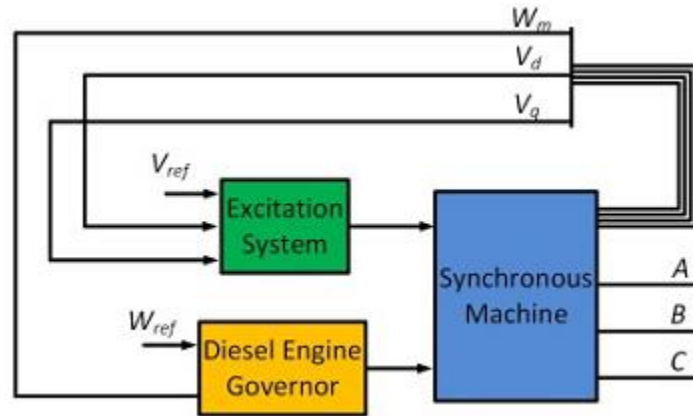


Fig. 3.4 Diesel generator model

3.1.1 PV Array Model

Two parallel PV arrays are used, each array has 14 panels and each panel includes 60 cells. The PV array output power is not given much consideration since the PV arrays are modeled as controlled voltage sources to facilitate the PV converter/inverter control.

Partial shading may occur during the operation of the panels which is not included in this paper but can be integrated as needed. Fig. 4 provides a model of one array.

Perturbation and observation (P&O) method is used to perform maximum power point tracking (MPPT) and a current sink is utilized as constant by which the buck converter can regulate the duty ratio to track the maximum power point.

The output voltage of the PV array is modeled as

$$V_{PV} = \frac{A \times K \times T}{q} \log\left(\frac{I_{lg} - I_{PV}}{I_0} - 1\right) - I_{PV} \times R_s \quad (3.1)$$

where A is diode-ideality factor, K is Boltzmann constant, T is absolute temperature, q is the basic charge, I_{lg} is light generated current, I_0 saturation current, and R_s is series resistance.

The output power is,

$$P_{PV} = I_{PV} \times V_{PV} \quad (3.2)$$

The P&O method regulates the duty cycle of the buck converter to track the maximum power point by comparing the old and new voltage and power being sampled as shown in Fig. 3.5

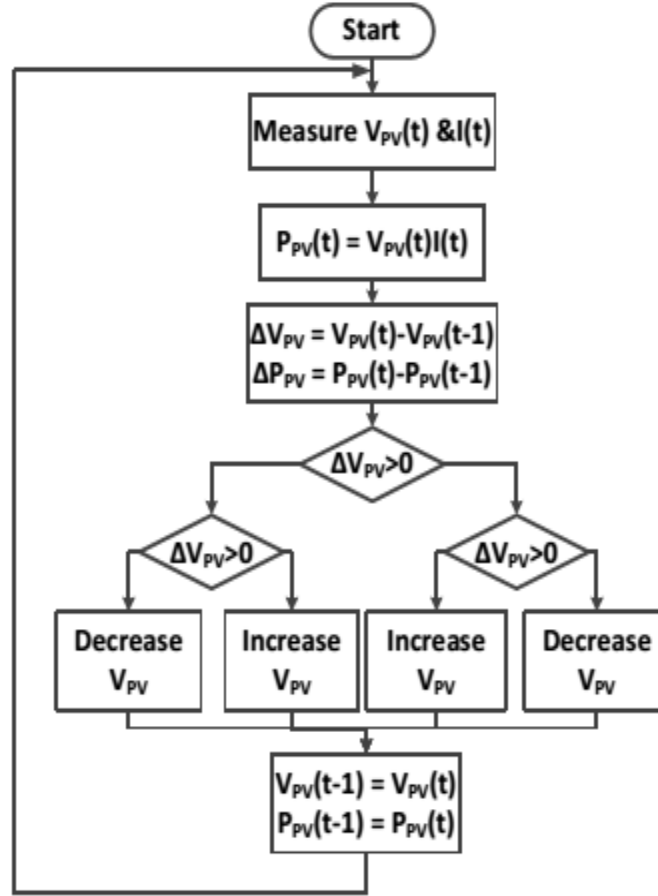


Fig. 3.5 Perturbation and observation method

The output voltage of the PV system is 430V DC and is controlled by a buck converter through a basic closed-loop voltage control to maintain a 350V DC into a three phase inverter.

On the grid side, a Y-Δ three phase transformer connects to the grid.

3.1.2 Fuel Cell Model

For the fuel cell, a polymer electrolyte membrane (PEM) fuel cell is used. PEM fuel cells have the advantages of operating at a low temperature, high power density, fast response and low emissions. They convert chemical energy of hydrogen and oxygen reactions into electrical energy. This paper models the fuel cell by assuming the hydrogen, oxygen, initial current and temperature are

constant values , and losses are modeled as steady/dynamic state activation loss, ohmic loss and concentration loss as shown in Fig. 3.3 The model of a fuel cell can be represented by open circuit voltage E . The output voltage of the fuel cell is thus,

$$V_{fc} = E - V_{act} - V_{ohm} - V_{con} \quad (3.3)$$

The open circuit voltage is obtained as

$$E = 1.229 - 8.5 \times 10^{-4}(T - 298.15) + 4.308 \times 10^{-5} T (\ln PH_2 + 0.5 \ln PO_2) \quad (3.4)$$

The activation loss is

$$V_{act} = -0.9514 + 3.12 \times 10^{-3} T - 1.87 \times 10^{-4} T \ln I + 7.4 \times 10^{-5} T (\ln PH_2 + 0.5 \ln PO_2) \quad (3.5)$$

The ohmic loss is

$$V_{ohm} = -IR_{int} \quad (3.6)$$

The concentration loss is

$$V_{ohm} = -IR_{int} \quad (3.7)$$

where T is cell temperature, I is current, I_{lim} is limit current and B is 0.016. In equations (4) and (5), the partial pressures of hydrogen and oxygen are

$$P_{H_2} = 0.5 P_{H_2O}^{sat} \left[\exp\left(-\frac{1.635I}{A T^{1.334}}\right) \frac{P_a}{P_{H_2O}^{sat}} - 1 \right] \quad (3.8)$$

$$P_{O_2} = P_{H_2O}^{sat} \left[\exp\left(-\frac{4.192 I / A}{T^{1.334}}\right) \frac{P_c}{P_{H_2O}^{sat}} - 1 \right] \quad (3.9)$$

The concentration of oxygen can be obtained by

$$C_{O_2} = \frac{P_{O_2}}{5.08 \times 10^{-6}} \exp\left(\frac{498}{T}\right) \quad (3.10)$$

while the saturation pressure of water is calculated by

$$\log_{10} P_{H_2O}^{sat} = -2.18 + 2.95 \times 10^{-2} T_c - 9.18 \times 10^{-5} T_c^2 + 1.44 \times 10^{-7} T_c^3 \quad (3.11)$$

Where $T_c = T - 273.15$

The internal resistance is

$$R_{int} = 1.605 \times 10^{-2} - 3.5 \times 10^{-5} T + 8 \times 10^{-5} I \quad (3.12)$$

For the dynamic model, the equation of the transient activation loss is

$$\frac{dV_{act}^t}{dt} = \frac{I}{C} - \frac{V_{act}^t}{R_a C} \quad (3.13)$$

where C is the charge double layer capacitance, R_a is the equivalent resistance:

$$R_a = \frac{V_{con} - V_{act}}{I} \quad (3.14)$$

3.1.3 Diesel Generator Model

The diesel generator model consists of three parts: diesel engine governor, excitation system and synchronous machine .

The excitation system provides the initial magnetic field to startup the synchronous machine, while the diesel engine governor utilizes a feedback mechanism to regulate and maintain the speed as needed to maintain electrical frequency by setting the reference speed w_f . The on and off state of the diesel engine can be controlled.

The diesel generator model contains two main parts: Diesel engine governor and synchronous generator. The structure of the diesel engine governor is shown in Fig. 3.6.

The PI controller and actuator are modeled by transfer functions with time constant $\tau_1, \tau_2, \tau_3, \tau_4$ and PI parameters K_i and K_p .

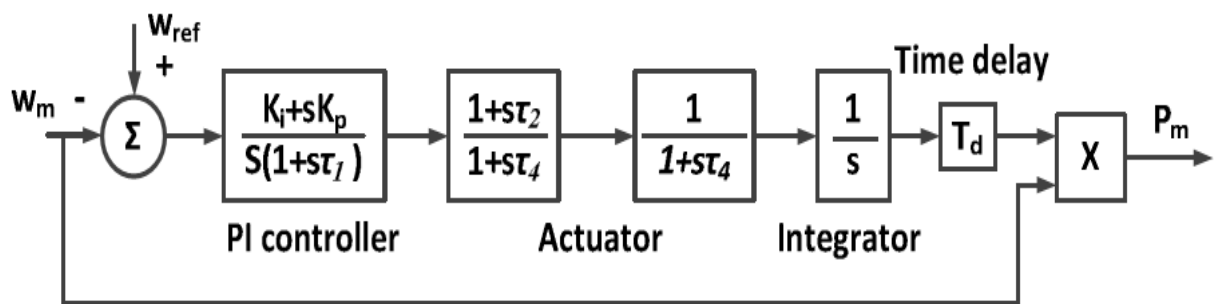


Fig. 3.6 Diesel engine governor model

The synchronous machine model considers the dynamics of the stator and field circuits:

$$L_s \frac{di_s^d(t)}{dt} = -r_s i_s^d(t) + w_e(t) L_s i_s^q(t) - v_s^d(t) - L_m \frac{di_f(t)}{dt} \quad (3.15)$$

$$L_s \frac{di_s^q(t)}{dt} = -r_s i_s^q(t) - w_e(t) L_s i_s^d(t) - v_s^q(t) - w_e(t) L_m i_f(t) \quad (3.16)$$

$$L_f \frac{di_f(t)}{dt} = -r_f i_f(t) + v_f(t) - L_m \frac{di_d(t)}{dt} \quad (3.17)$$

where i_s^d , i_s^q and V_s^d , V_s^q are stator currents and voltages in dq reference frame; r_s is stator resistance, L_s is stator inductance; i_f , V_f are field excitation current and voltage.

The inductance of the field excitation circuit is L_f , the mutual inductance between the field circuit and the d axis of the stator is L_m . w_e is the electrical angular frequency and can be represented as:

$$w_e = N_{pp} w_r \quad (3.18)$$

where w_r is the speed of the rotor, N_{pp} is the number of pole pairs.

The diesel generator is a standby power source to supply the power system in the event when clean energy generation systems cannot produce sustainable power in island mode, or when the grid should be disconnected due to irregular voltage or frequency.

3.2 Inverter control and synchronization

Closed-loop control is also applied to three phase inverter, different from classic PI control where the inverter output and balanced three-phase reference signals are synchronized as shown in Fig. 3.7.

To maintain this reference when the grid is lost, a synchronized source shown in Fig. 3.8 is generated from the grid and synchronizes all necessary parameters, especially phase information, for all inverters on the micro-grid.

After one cycle from the simulation start time, selection switches shown in Fig. 3.7 switch to replace the utility grid generated ω_t to create stand-alone sinusoidal control waveforms.

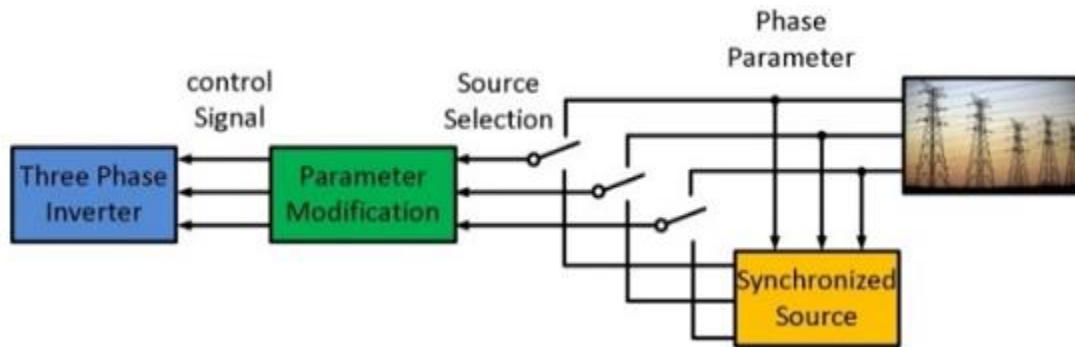


Fig. 3.7 Closed-loop control for three phase inverter

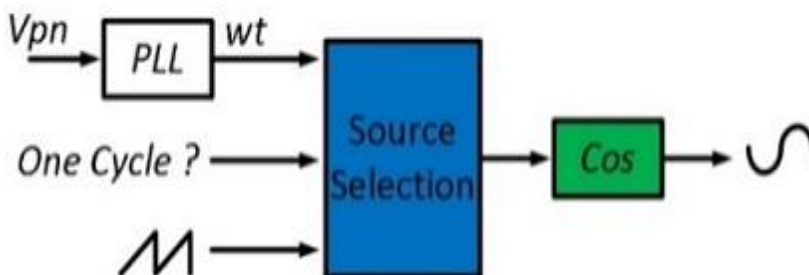


Fig. 3.8 Synchronized source

Note that the models developed in the paper address a specific implemented micro-grid but other models can be integrated to the micro-grid simulation for more generation and load options.

The main purpose of the models presented here is to achieve a robust and flexible real-time simulation platform for further research and development while capturing fast and slow dynamics in addition to control effects.

CHAPTER 4

PROPOSED METHOD

4.1 Introduction

A new topology of a hybrid distributed generator based on photovoltaic, wind-driven permanent magnet synchronous generator and fuel cell is proposed. In this generator, the sources are together connected to the grid with the help of only a single boost converter followed by an inverter. Contrary to earlier schemes, the proposed hybrid generator has a PV array being directly connected to the DC link instead of being connected through a DC-DC converter. The DC link voltage is varied by a DC-DC converter interposed between the rectifier fed by PMSG and the grid connected inverter. The output voltage of the DC-DC converter forms the load line for the PV array. The inverter current is varied to extract maximum current from both the sources using current control strategy. The proposed topology could thus dispense with a DC-DC converter, which in earlier schemes were connected after the PV array for maximum power extraction. Two new controllers are attempted for the hybrid scheme proposed, in order to achieve the maximum power extraction from all three sources. A d-qaxes model of the scheme has been developed and validated. The successful operation of this scheme in extracting maximum power from both the sources or from each of the sources has been established through simulation and experimental investigations. Further, the proposed scheme is also for employment by domestic consumers in a smart grid scenario, and hence maintenance free simple operation is envisaged. The proposed scheme is for a grid connected operation and hence battery storage is not necessary.

4.2 Proposed DG scheme

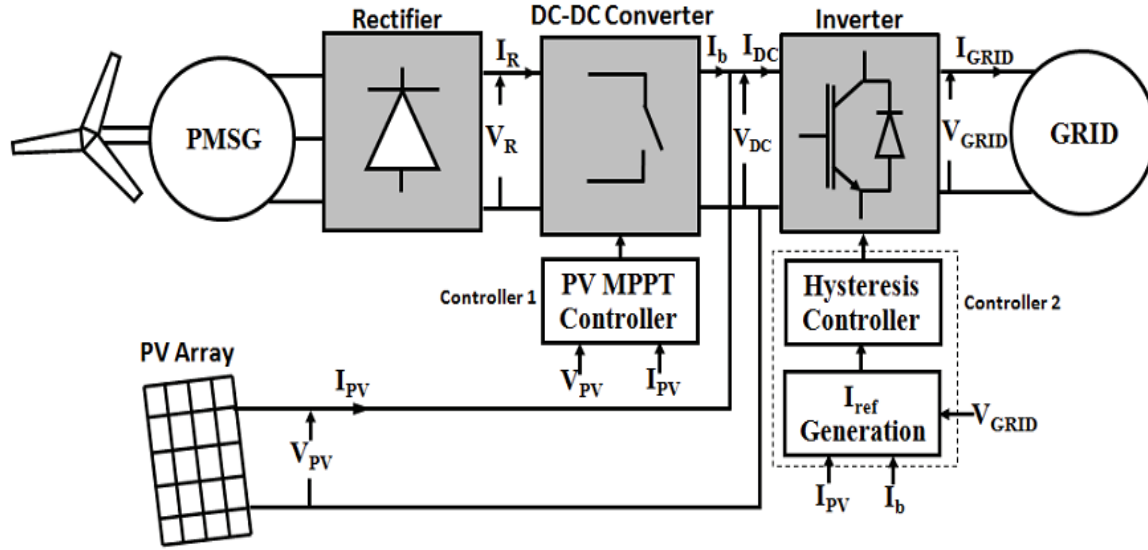


Fig. 4.1 Proposed DG system based on Wind-PV sources

The block diagram of proposed DG scheme is given in Fig. 4.1, where a direct driven PMSG and a PV array are the sources. The PMSG output is rectified and fed into a DC-DC boost converter. The rectifier output voltage varies with the wind-speed. The PV array terminals are connected to the output of the DC-DC converter to form a common DC link for the proposed system. The inverter input terminals are tied to this common DC link. The PV array voltage (V_{PV}) is fixed to the output voltage of the DC-DC converter (V_{DC}) since the output terminals of both the PV array and the DC-DC converter are tied together. The output voltage of the DC-DC converter is automatically varied by a PV MPPT controller (Controller 1) to PV array's maximum power point voltage. Under this condition, the maximum current for the given irradiation is drawn from the PV array by the action of current controller (controller 2) of the inverter. The basic Perturb & Observe (P&O) algorithm is employed with an inverted duty-cycle adjustment in controller 1. This

revised adjustment in the proposed scheme is because of the DC-DC boost converter being fed by a stiff DC source (rectifier output) instead of the PV array. The output voltage of the current controlled inverter is tied to the grid voltage and the frequency and the phase requirement for synchronization are automatically met. The current fed to the grid by the inverter (I_{GRID}) follows the reference current signal (I_{ref}), which is automatically varied by controller 2 for drawing the maximum current from both PMSG & PV array. In the proposed scheme, the setting of DC voltage reference of the DC-DC converter to the peak power point voltage of the PV array and the reference current setting of current controlled inverter corresponding to the maximum current extractable from both the sources, results in peak power extraction from both the sources.

4.3 Maximum Power Point Tracking algorithms

4.3.1. Hill Climb Search (HCS) method

HCS method of MPPT makes use of the inverted U shaped graph between power and rotor speed. As there is a definite peak power corresponding to a particular rotor speed, the algorithm compares the present power at an instant to the power obtained at the previous step. If the power is found to be increasing, then the duty cycle of the gating pulse applied to the converter switches are increased to drive the operating point more towards the peak power. If the power is found to be decreasing, then the duty cycle is reduced. The primary advantage of this method is its simplicity and independence from wind turbine characteristics. A severe limitation of the HCS method is its inability to track the maximum power point in cases of abruptly varying wind conditions. In normal HCS methods the increments/decrements given to the duty cycle are fixed.

4.4 Model of the proposed system

A model of the proposed DG system is developed to investigate the system performance. PMSG has been described by its steady state equivalent circuit and is shown in Fig. 4.2. The rectifier DC output voltage (V_R) and current (I_R) in terms of stator phase voltage V_s (rms) and stator current I_s (rms) are given as

$$V_R = \frac{3\sqrt{6}}{\pi} V_s \quad (4.1)$$

$$I_R = \frac{\pi}{\sqrt{6}} I_s \quad (4.2)$$

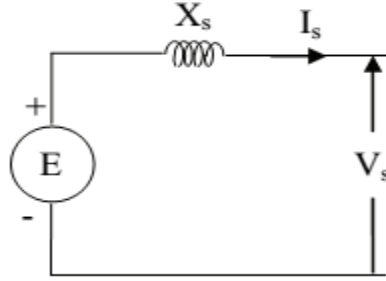


Fig. 4.2 Per-phase steady state equivalent circuit of PMSG

V_s vary with wind-speed and hence the rectifier output voltage V_R is a varying DC. This varying DC feeds the DC-DC converter. The output voltage of the DC-DC converter is given as

$$V_b = V_{DC} = V_R \frac{1}{1-\delta} \quad (4.3)$$

The DC link current is

$$I_{DC} = I_b + I_{pv} \quad (4.4)$$

and the PV array current (I_{PV}) is given by

$$I_{PV} = I_{SC} - I_d \quad (4.5)$$

Where

$$I_d = 10^{-9} I_{SC} \left(\exp \frac{20.7}{V_{OC}} (V_{PV} + R_{se} I_{PV}) \right) \quad (4.6)$$

The d-axis and q-axis voltage of the inverter are related with the DC link voltage as,

$$v_d = V_{DC} g_d \quad (4.7)$$

$$v_q = V_{DC} g_q \quad (4.8)$$

Where

$$g_d = \left[\begin{aligned} & \sum_{n=1,5,9...} \cos(n-1)\omega t - \sum_{n=3,7,11...} \cos(n+1)\omega t \\ & + \left(\sum_{n=2,6,10...} \frac{1}{\sqrt{2}} \left\{ \cos \left[(n-1)\omega t - \frac{\pi}{4} \right] + \cos \left[(n+1)\omega t - \frac{3\pi}{4} \right] \right\} \right) \\ & + \left(\sum_{n=4,8,12...} \frac{1}{\sqrt{2}} \left\{ \cos \left[(n-1)\omega t + \frac{\pi}{4} \right] - \cos \left[(n+1)\omega t - \frac{\pi}{4} \right] \right\} \right) \end{aligned} \right] \quad (4.9)$$

$$g_q = \left[\begin{aligned} & \sum_{n=1,5,9...} \sin(n-1)\omega t - \sum_{n=3,7,11...} \sin(n+1)\omega t \\ & + \left(\sum_{n=2,6,10...} \frac{1}{\sqrt{2}} \left\{ \cos \left[(n-1)\omega t - \frac{3\pi}{4} \right] + \cos \left[(n+1)\omega t - \frac{\pi}{4} \right] \right\} \right) \\ & + \left(\sum_{n=4,8,12...} \frac{1}{\sqrt{2}} \left\{ \cos \left[(n-1)\omega t - \frac{\pi}{4} \right] + \cos \left[(n+1)\omega t - \frac{3\pi}{4} \right] \right\} \right) \end{aligned} \right]. \quad (4.10)$$

Considering zero power loss in the inverter,

$$I_{DC} = \frac{1}{2}(i_d g_d + i_q g_q) \quad (4.11)$$

Assuming zero power loss in DC-DC converter,

$$V_R I_R = V_b I_b \quad (4.12)$$

and

$$I_{DC} = I_b + I_{pv} = (1 - \delta)I_R + I_{pv} = \frac{(1 - \delta)\pi}{\sqrt{6}} I_S + I_{pv} \quad (4.13)$$

Where δ is duty-cycle of the DC-DC converter. The rectifier output (3.23) is connected to the models of DC-DC converter, PV array and the inverter. The d axis and q axis circuits of the system are shown in Fig. 4.3 and Fig. 4.4 respectively.

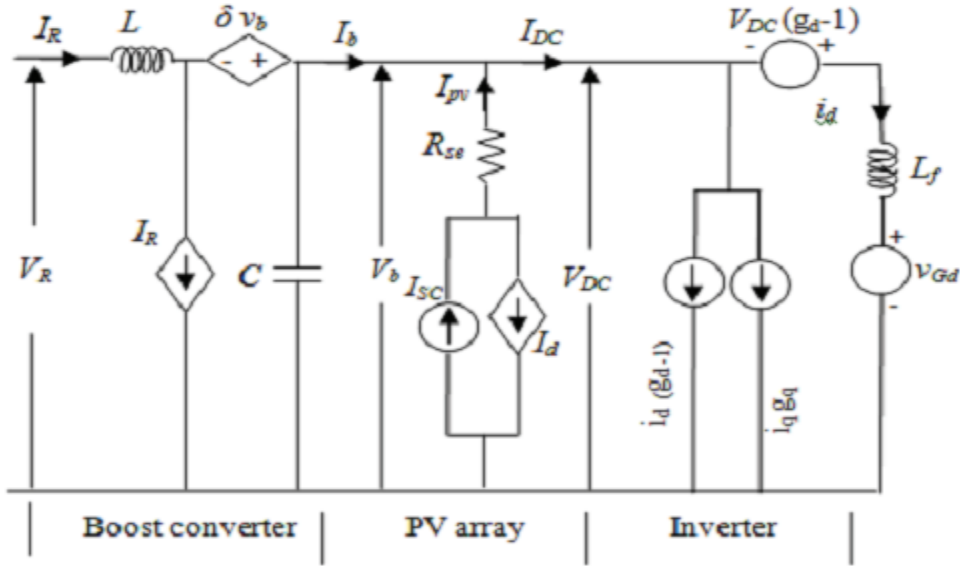


Fig. 4.3 d-axis equivalent of the system

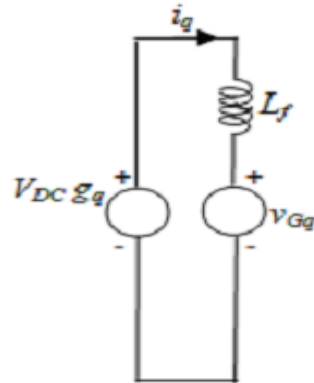


Fig. 4.4 q-axis equivalent of the system

In the proposed scheme, δ and I_{ref} are varied to extract the maximum I_{DC} at any instant of time. Using Equations (4.1)-(4.13), the proposed DG system can be simulated on any platform. MATLAB has been employed to simulate the proposed scheme in this project.

4.5 Operation of the Controllers

4.5.1. Case 1 (PV and PMSG generating power)

The wind and solar sources are generating power together in this case and the variation of duty-cycle of the DC-DC converter will eventually disturb the PV array's terminal voltage (since $V_{DC} = V_{PV}$). The rectifier voltage varies with the wind-speed and the duty-cycle of the boost converter needs to be automatically adjusted such that V_{DC} is equal to the peak power point voltage (V_m) of the PV array. At this point ($V_{PV} = V_{DC} = V_m$), the PV array delivers the maximum current (I_m) which is concurrently drawn by the current controlled inverter. The DC link voltage may be, say $V_1(B)$ or $V_2(C)$ depending upon the present duty-cycle of the DC-DC converter. To operate the PV array at its maximum power point (A), the DC-DC converter output (DC link voltage) is adjusted to V_m by varying the duty-cycle of the DC-DC converter by controller1. The duty-cycle variation of controller 1 is given by

$$\delta_{new} = \delta_{old} + \text{sgn}(\Delta P) \text{sgn}(\Delta V_{PV}) \Delta \delta \quad (4.14)$$

Where $\Delta \delta$ is the perturbation in duty-cycle, sgn is Signum function. ΔP is the difference in PV array power and ΔV_{PV} is difference in PV array voltage before and after perturbation. If ΔP and ΔV_{PV} are both either positive or negative then the duty-cycle increases and vice-versa if different. The duty cycle variation in this scheme is hence exactly opposite to the duty-cycle variation of a P&O controller used in existing schemes, where a PV array precedes a boost converter.

The main objective of controller 2 shown in Fig. 4.1 is to vary the inverter output current fed to the grid. The reference current (I_{ref}) for this hysteresis current controller is derived based on the available maximum power from the both the

sources for a particular condition (i.e. irradiation and PMSG shaft torque). V_{PV} , is at maximum power point value by the action of controller 1. Current drawn from the boost converter (I_b) and P_v (I_{PV}) together is maximized by changing I_{ref} as

$$I_{ref(new)} = I_{ref(old)} + \text{sgn}[\Delta(I_{PV} + I_b)]K \quad (4.15)$$

Where $\Delta(I_{PV}+I_b)$ is the change in the sum of I_{PV} and I_b and K is the step in perturbation of I_{ref} . It is clear from (4.15), if current to be drawn from boost converter increases, I_{ref} also increases correspondingly.

At steady-state, the reference current value for a particular condition of irradiation and wind speed is

$$I_{ref} = \sqrt{2}(V_{PV}I_{PV} + V_R I_R) / V_{GRID} \quad (4.16)$$

4.5.2. Case 2 (PMSG alone generating power)

It is obvious that during night time, the current transducer connected to the PV terminal will not give any response. In such a case, the controller 1 will skip the PV-MPPT algorithm and work in a voltage control mode. By taking the voltage transducer output (V_{DC}) as feedback signal, the controller 1 varies the duty-cycle of the boost converter to maintain the DC link voltage to a DC value corresponding to the rated RMS voltage of the grid. As I_{PV} is zero in this case, the controller 2 will keep adjusting the (I_{ref}) such that [by substituting $I_{PV} = 0$ in (4.15)]

$$I_{ref(new)} = I_{ref(old)} + \text{sgn}[\Delta(I_b)]K \quad (4.17)$$

to extract the maximum power from the PMSG alone.

4.5.3. Case 3 (PV alone generating power)

When PMSG is not generating power, there is no input to the DC-DC converter and hence no triggering pulse is generated by controller 1. The controller 2 varies I_{ref} such that [by substituting $I_b = 0$ in (4.3)] to feed the maximum power from PV array alone.

$$I_{ref(new)} = I_{ref(old)} + \text{sgn}[\Delta(I_{PV})]K \quad (4.18)$$

4.5.4. Composite operation of controllers

It is evident from all the three cases explained above, that controller 2 functions always to feed the maximum power either from both the sources or from any one of the sources to the grid by adjusting I_{ref} . On the other hand, controller 1 is idle when power is generated by PV alone. Different status of sources and the corresponding functions of two controllers are summarized in Table. 4.1.

Table 4.1 Functions of controllers under different conditions

Sources	Controller for DC-DC converter (Controller 1)	Hysteresis Controller (Controller 2)
PV and PMSG	Generates duty-cycle for PV array MPPT voltage	Generates current command to extract the maximum power from both the sources
PV alone	Triggering pulse not generated (Zero duty-cycle)	Generates current command to extract the maximum power from PV
PMSG alone	Generates duty-cycle to maintain constant DC link voltage*	Generates current command to extract the maximum power from PMSG

* Corresponding to the RMS voltage of the grid

4.6 Implementation of the Controllers

4.6.1. Controller for DC-DC Converter (Controller 1)

PIC 16F876A, a very low cost 16 bit microcontroller from MICROCHIP is used to implement the controller for the DC-DC converter. This controller gets feedback signals from a voltage transducer (LV20-P) and a current transducer (LA50-P) connected to the PV array terminals.

The signals from these transducers are processed by signal conditioning circuits (SCC) and then connected to analog inputs of the microcontroller. These signals are digitized through internal Analog to Digital Conversion (ADC) module.

The microcontroller is programmed to perform the MPPT algorithm for PV array based on (3.36). In built pulse width modulation (PWM) module of the microcontroller is enabled to produce the required PWM pulses for DC – DC converter.

4.6.2. Hysteresis Current Controller (Controller 2)

The complete schematic of controller 2 is given in Fig. 4.1. High frequency op-amps (LM-318) are used to construct the hysteresis-current-controller. I_{PV} and I_b are sensed by the current transducers and digitized by the internal ADC module of the microcontroller.

Based on (4.15), I_{ref} is determined and available as digital output from the microcontroller. This digital value is subsequently processed by a Digital to Analog Conversion (DAC) IC to obtain a DC value which corresponds to the peak value of I_{ref} . This DC value is multiplied with the sine wave reference extracted from the grid voltage, by a multiplier IC and fed to the hysteresis- current-controller as the reference current signal.

When PV array (or PMSG) alone generates power, I_b (or I_{PV}) will be zero and I_{ref} is perturbed and adjusted automatically to extract the maximum power from PV array (or PMSG).

When both the sources are generating, I_{ref} will be perturbed based on (4.15) and adjusted to maximize the DC link current I_{DC} for the corresponding irradiation and wind-speed conditions.

As the sine wave reference is taken from the grid, the inverter output current will have grid frequency and will be in phase with the grid voltage.

CHAPTER V

RESULT AND DISCUSSIONS

In order to validate the performance of the proposed converter and the grid connected system, this project is designed with a wind generator system and voltage controller along with the grid connected control system that maintains the dc link voltage based on the PQ transform, the grid voltage and current are synchronized through the inverter which stabilizes the link dc voltage. In order to verify the performance of the proposed single converter system a model based on MATLAB /Simulink is designed and the experimental waveforms are obtained.

5.1 Existing method

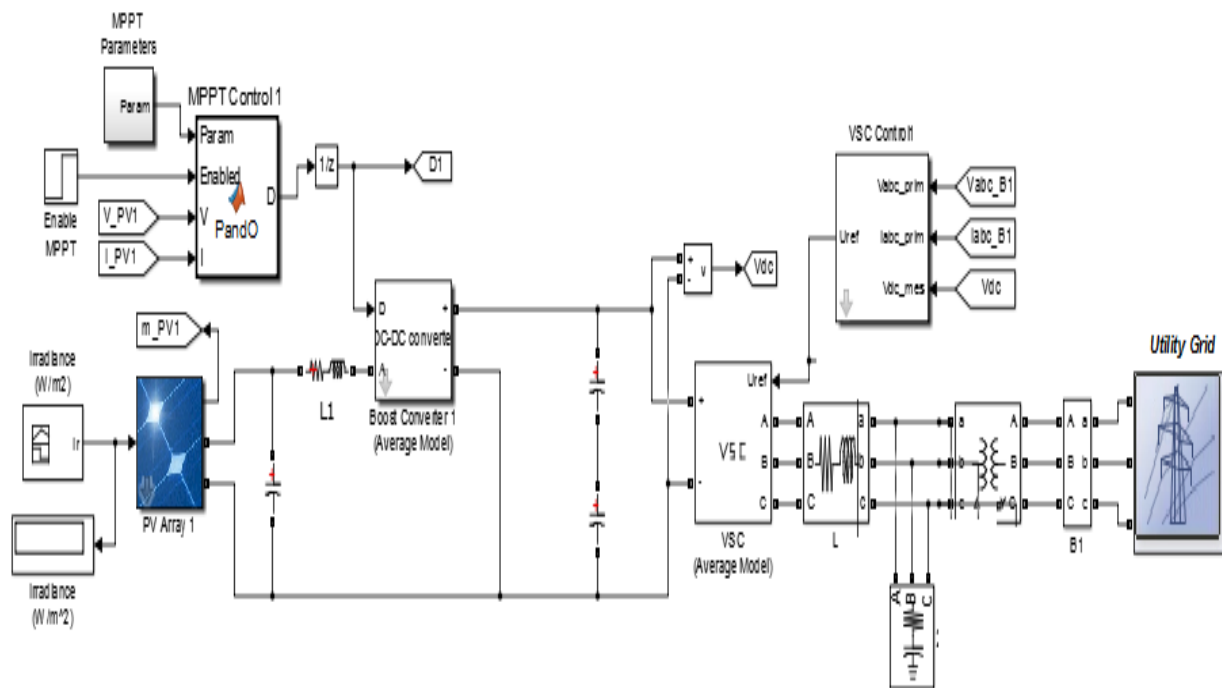


Fig. 5.1 Simulation model contain PV, DC-DC converter and utility grid

The proposed simulation model of the grid connected wind, PV and fuel cell generations consists a solar and the wind power generators, in that, wind generator is connected to the dc-dc converter followed by a solar which is connected to the dc link capacitor, the speed of the wind turbine and energy generated from the solar panel are taken in account and analyzed and this is shown in Fig. 5.2.



39

shows the wind model connected to the 3phase rectifier, DC-DC boost converter used in Pitch control to extract maximum power from it.

40

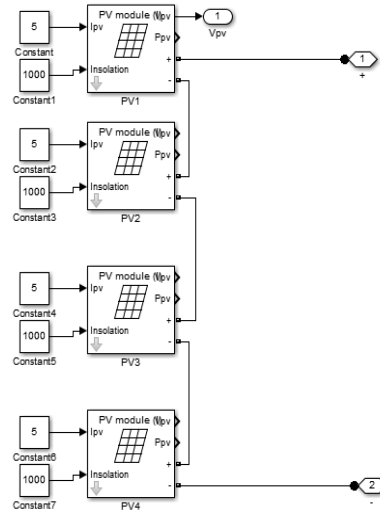


Fig. 5.4 MATLAB simulation of PV Model

The property of PV panels which are used in the proposed model is shown in the Fig. 5.5 and the property of single PV module used in the proposed system is shown in Fig. 5.6.

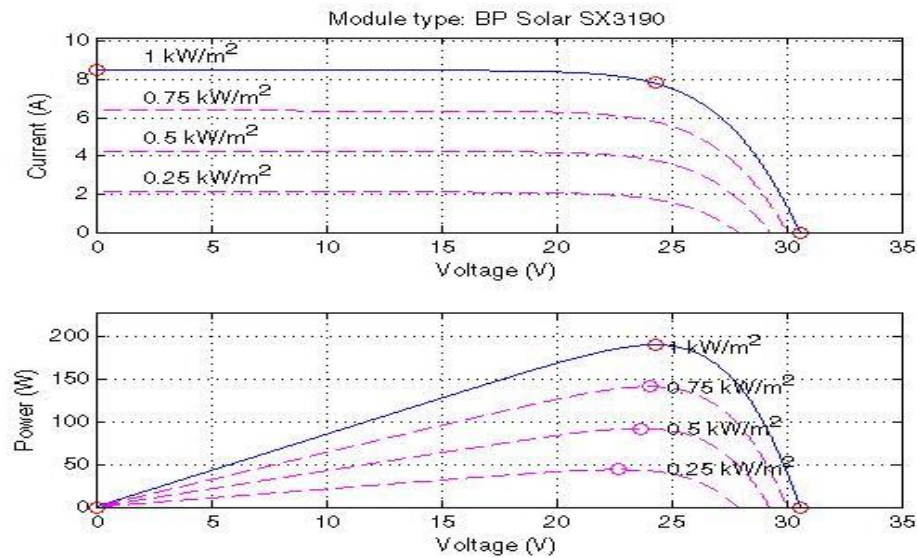


Fig. 5.5 PV panel properties

Figure shows the PV panel properties in V-I and P-V curve used in simulating the proposed work

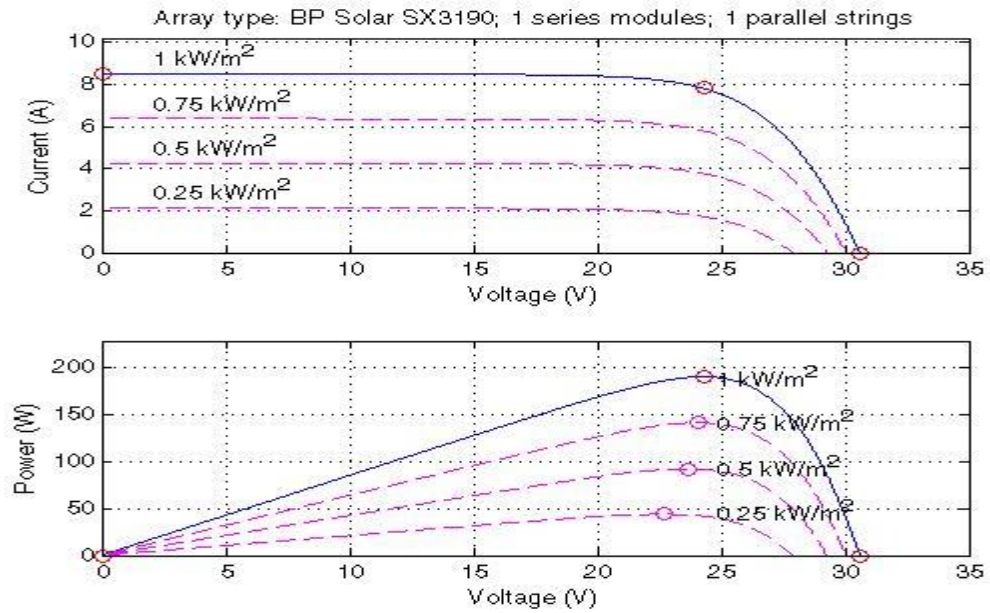


Fig. 5.6 Characteristics of a single module shows the characteristics of single module in I-V and P-V curve of the simulated panel

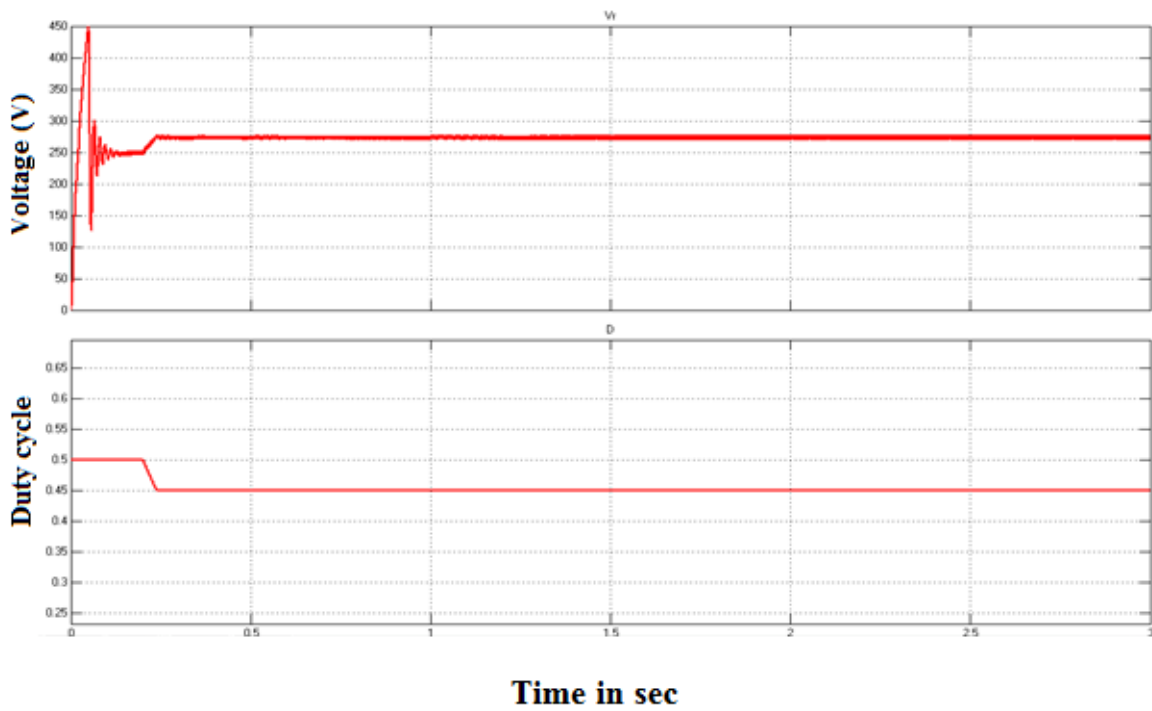


Fig. 5.7 Changes in rectifier output voltage and duty cycle of boost converter

For a step increase, the rectifier voltage level and duty-cycle of boost converter changes and is shown in Fig. 5.7.

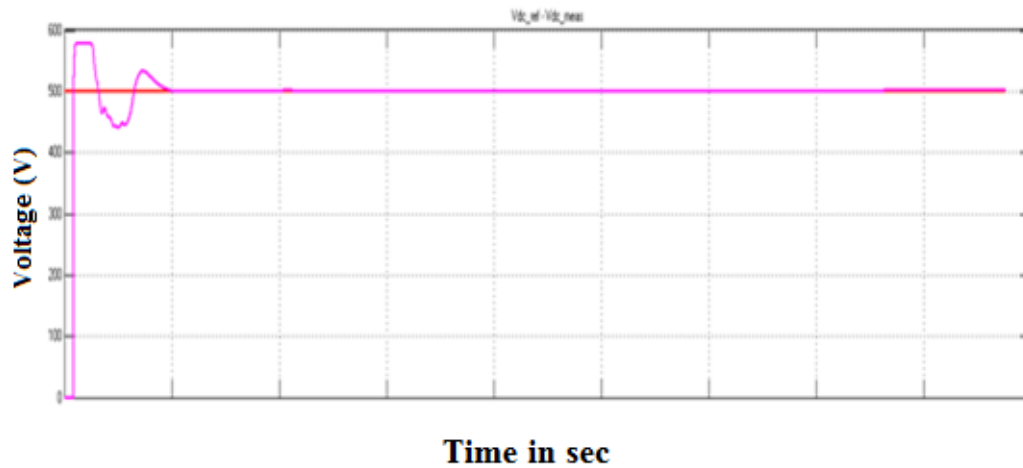


Fig. 5.8 DC link voltage control

The proposed controller efficiently tracks the set point voltage by varying the modulation index of the inverter which is shown in the figure below to the voltage control graph. As the voltage changes the dc tracking voltage variation of the system, it also changes the index which is fluctuating between 0.85 to 0.84 due to the variation of the boost converter the dc link voltage would tend to change, as the composite controller is linked with the dc link voltage it generates the required control signal to adjust the grid voltage and maintains the dc link to reference, by varying the inverter triggering signals through the variation of the modulation index. Fig. 5.8 shows the dc link voltage control by the controller 2 which is responsible to maintain the dc link voltage.

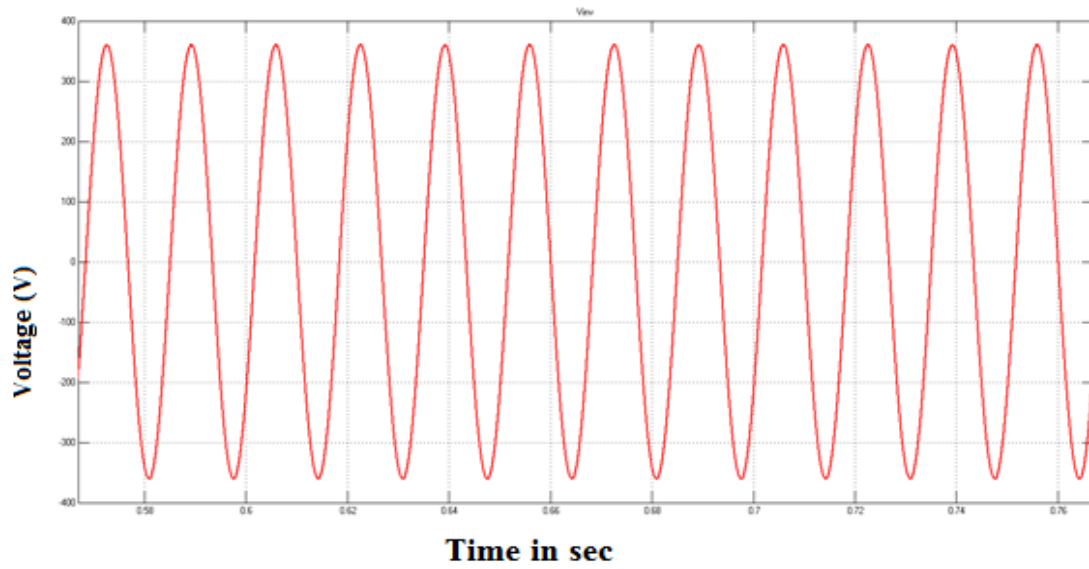


Fig. 5.9 Inverter output voltage

Fig. 5.9 depicts the inverter voltage which is the output of inverter converted from DC to AC. The converted AC voltage is filtered for harmonics reduction and then it is synchronized into the grid.

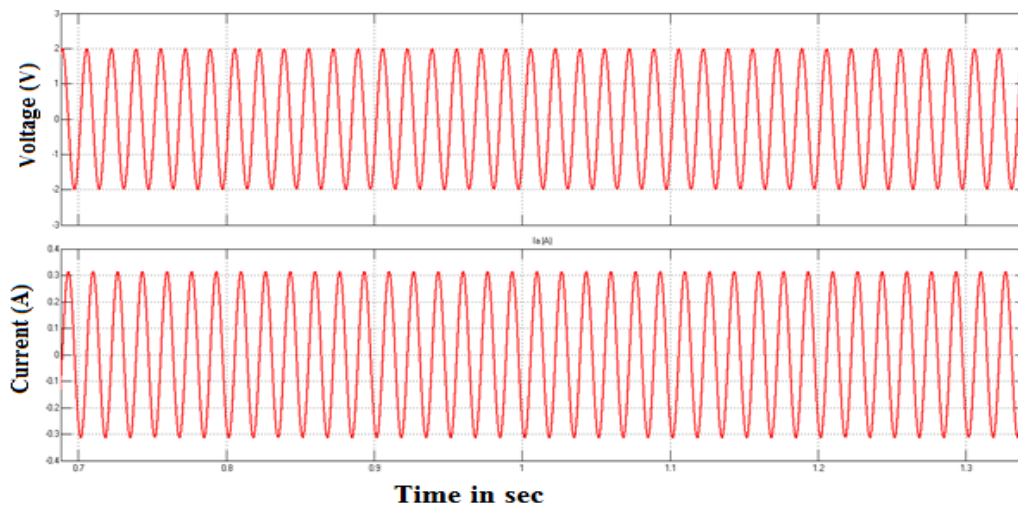


Fig. 5.10 Steady-state grid voltage and current waveforms

The current was delivered to the grid by the inverter at unity power factor. Grid voltage and current of the proposed grid connected system represents the voltage and current are maintained as inline by the controller 2 and this shown in Fig. 5.10 From the simulated results, we can able to analyze the THD for grid voltage and current and are shown in Fig. 5.11 and Fig. 5.12.

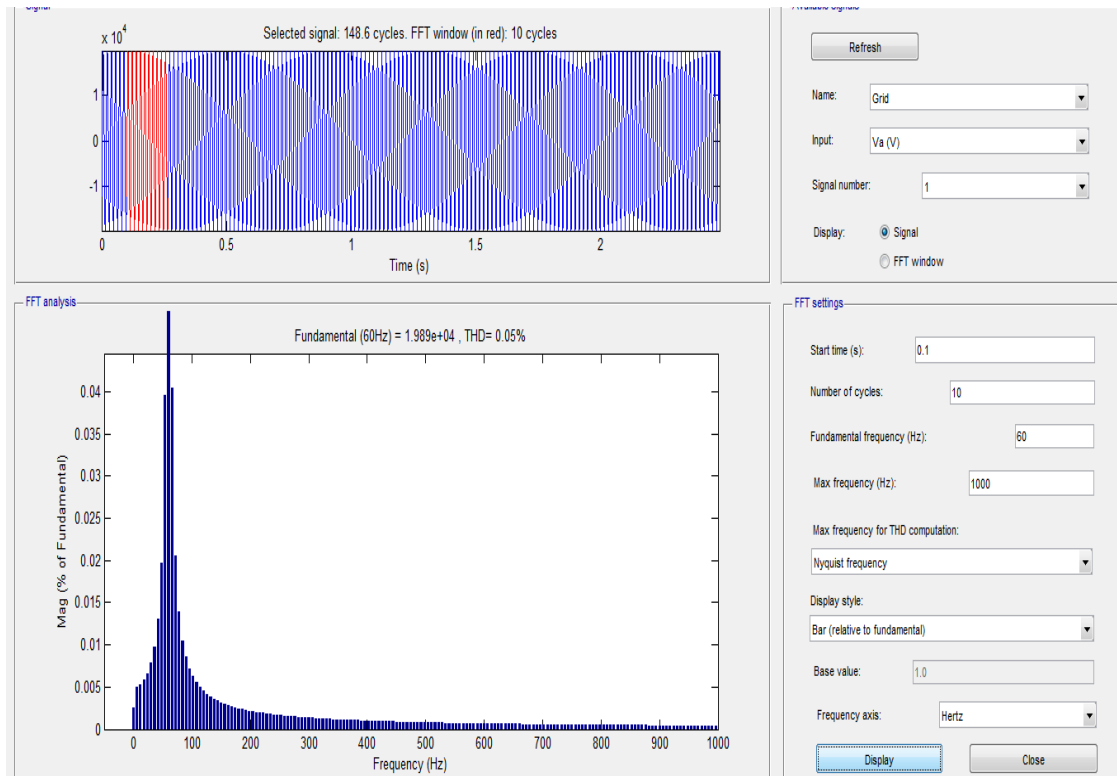


Fig. 5.11 Harmonic analysis of grid voltage

Fig 5.11 show the harmonics of output voltage find through FFT analysis. It has 0.05%.

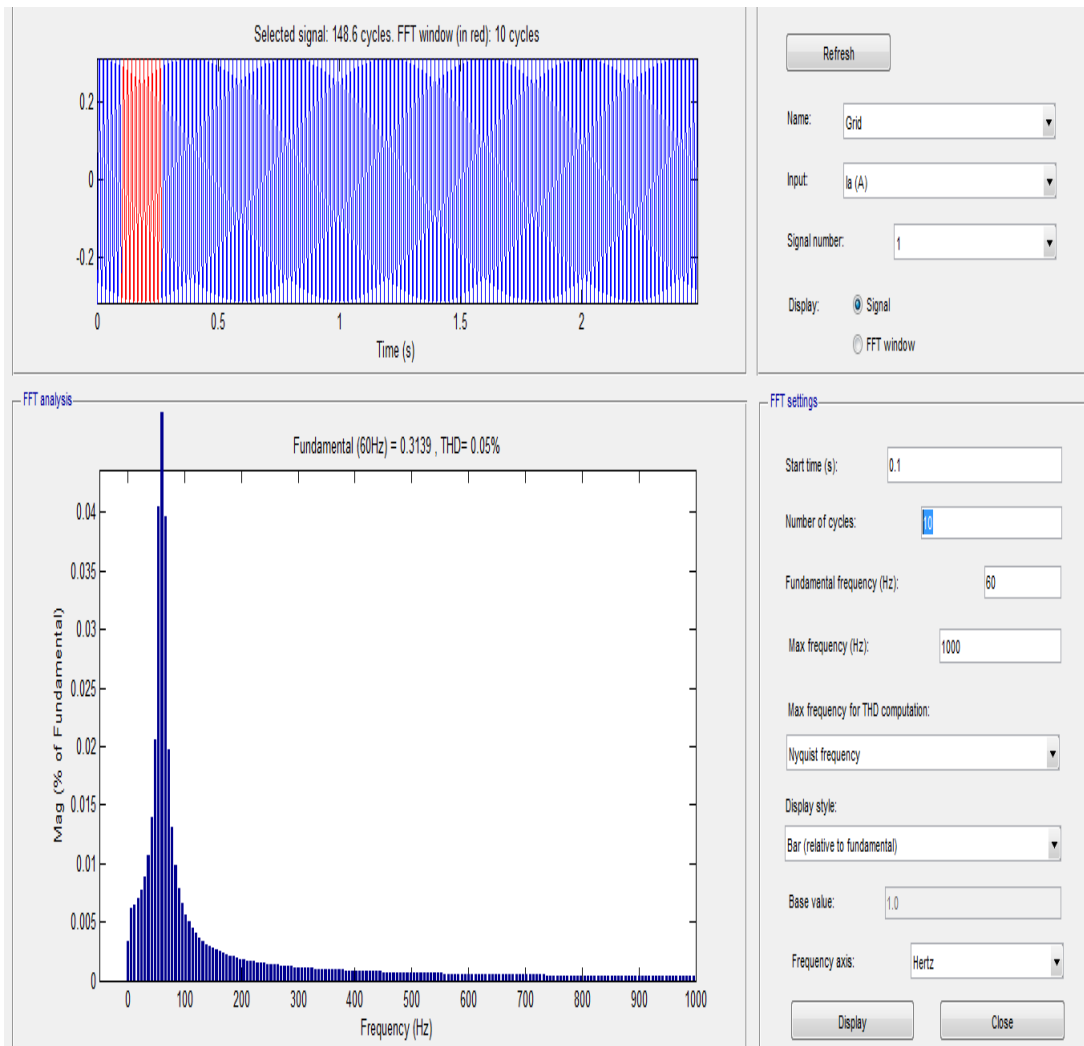


Fig. 5.12 Harmonic analysis of grid current

The total harmonic distortion (THD) of the voltage and the current at grid side were measured by using FFT analyzer and the results are shown in above Fig. 5.11 and 5.12.

5.3 Comparison Between Existing System And Proposed System:

Existing System	Proposed System
Harmonic reduction are not improved	Harmonic reduction are improved
Different sources and different potential are not synchronized	Different Sources and different potential are synchronized
Fuel cell is not implemented	Fuel Cell is implemented
Common reference control is existed	Voltage and Current reference control is proposed
Dc grid control is absent in existing system	Dc grid control is present in proposed system

CHAPTER 6

CONCLUSION AND FUTURE SCOPE

6.1 Conclusion

The design of an micro-grid with multiple renewable sources are been constructed , the multiple dc sources are able to synchronize to grid based on the single synchronizing control , the voltage balancing among the sources are being controlled to generate a unity grid voltage scheme , both the grid connected and the islanding schemes are validated , in the base scheme each renewable system is connected to grid through a numerous of conversions which requires a higher level of control requirements which cannot be reduced in a total control system addition of a larger control scheme could result in higher cost and local coordination is required to manage the loads.

In order to reduce the control complexity a new reliable hybrid DG system based on PV and wind driven PMSG as sources, with one boost converter followed by an inverter stage, has the two controllers, MPPT controller and hysteresis-current-controller which are designed specifically for the proposed system have exactly tracked the maximum powers from both the sources.

The proposed configuration is simpler and easier to tie multiple of the hybrid renewable systems without any further addition of control scheme. The steady state waveforms captured at grid-side of the proposed hybrid system shows that power generated by the DG system is fed to the grid is near to the unity power factor and the voltage and current are in phase with each other than the output waveforms in the existing system. It also shows less harmonics in output voltage and current.

6.2 Future Scope

A microgrid configuration with multiple dc sources are being implemented in this the topology of the renewable sources to grid with the PV, fuel cell and the wind power are being modified with a single controller and they are being able to track to their maximum power points to a satisfactory level . In this configuration the renewable schemes of the with the differential mppt schemes are not validated.

More over the operating mpp levels of the various schemes are not being taken care , hence the extension of this work would be based on the integration and the operation control of multiple resources with the varying peak power and the extraction of the peak power.

PRESENTATION/PUBLICATION:

Presented “**DISTRIBUTED GENERATION SYSTEM USING HYBRID RENEWABLE ENERGY SOURCES**” in the International Conference on Power and Energy Systems (ICPES-23) organized by the Department of Electrical and Electronics Engineering, Velammal College of Engineering and Technology on 17th & 18th March 2023.





VELAMMAL COLLEGE OF ENGINEERING AND TECHNOLOGY
(AUTONOMOUS), MADURAI-625009

Accredited with NBA and NAAC with "A" Grade

DEPARTMENT OF ELECTRICAL AND ELECTRONICS ENGINEERING

Certificate of Participation

This is to certify that **Mr.V.BA.Jeyvishnu,UG Student , Velammal College of Engineering and Technology, Madurai** has presented a paper in the "International Conference on Power and Energy Systems (ICPES- 23)" organized by the Department of Electrical and Electronics Engineering, Velammal College of Engineering and Technology on 17 & 18 March 2023.

Dr.B.Kiruthiga
Organising Secretary

Dr.S.Chellam
Organising Secretary

Dr. R Narmatha Banu
HOD / EEE,VCET



VELAMMAL COLLEGE OF ENGINEERING AND TECHNOLOGY
(AUTONOMOUS), MADURAI-625009

Accredited with NBA and NAAC with "A" Grade

DEPARTMENT OF ELECTRICAL AND ELECTRONICS ENGINEERING

Certificate of Participation

This is to certify that **Mr.T.K.B.Vijay Krishna, G Student , Velammal College of Engineering and Technology, Madurai** has presented a paper in the "International Conference on Power and Energy Systems (ICPES-23)" organized by the Department of Electrical and Electronics Engineering, Velammal College of Engineering and Technology on 17 & 18 March 2023.

Dr.B.Kiruthiga
Organising Secretary

Dr.S.Chellam
Organising Secretary

Dr. R Narmatha Banu
HOD / EEE,VCET

REFERENCES

1. Barklund, E., Pogaku, N., Prodanovic, M., Hernandez-Aramburo, C., and Green, T. C., “Energy management in autonomous micro-grid using stability-constrained droop control of inverters,” *IEEE Trans. Power Electron.*, Vol. 23, p. 2346, 2016.
2. Bollen, M., Zhong, J., Samuelsson, O., and Bjoernstedt, J., “Performance indicators for microgrids during grid-connected and island operation,” *IEEE Bucharest Powertech*, Vol. 1–5, pp. 866–871, 2017.
3. Chen, Weiqiang, Ali M. Bazzi, James Hare, and Shalabh Gupta. "Real-time integrated model of a micro-grid with distributed clean energy generators and their power electronics." In *2015 IEEE Applied Power Electronics Conference and Exposition (APEC)*, pp. 2666-2672. IEEE, 2015.
4. Chung, I., Park, S., Kim, H., Moon, S., Han, B., Kim, J., and Hoi, J., “Operating strategy and control scheme of premium power supply interconnected with electric power systems,” *IEEE Trans. Power Delivery*, Vol. 20, No. 3, pp. 2281–2288, July 2018.
5. Guerrero, J. M., Hang, L., and Uceda, J., “Control of distributed uninterruptible power supply systems,” *IEEE Trans. Indust. Electron.*, Vol. 55, No. 8, pp. 2845–2859, August 2017.
6. Hao, J., Chen, C., Libao, S., and Jie, W., “Nonlinear decentralized disturbance attenuation excitation control for power systems with nonlinear loads based on the Hamiltonian theory,” *IEEE Trans. Energy Conversion*, Vol. 22, No. 2, pp. 316–324, 2015.
7. Hatziargyriou, N., Asano, H., Iravani, R., and Marnay, C., “Microgrids,” *IEEE Power Energy Mag.*, Vol. 5, No. 4, pp. 78–94, July/August 2018.

8. Katiraei, F., and Iravani, M. R., “Micro-grid autonomous operation during and subsequent to islanding process,” IEEE Trans. Power Delivery, Vol. 20, No. 1, pp. 248–257, January 2019.
9. Katiraei, F., and Iravani, M. R., “Power management strategies for a microgrid with multiple distributed generation units,” IEEE Trans. Power Syst., Vol. 21, No. 4, pp. 1821–1831, November 2017.
10. Lasseter, R. H., “Microgrids,” Proc. Power Eng. Soc. Winter Mtg., Vol. 1, pp. 305–308, January 2019.
11. Lopez, J. A. P., Moreira, C. L., and Madureira, A. G., “Defining control strategies for microgrid islanded operation,” IEEE Trans. Power Syst., Vol. 21, No. 2, pp. 916–924, May 2016.
12. Mohamed, Y., and El-Saadany, E. F., “Adaptive decentralized droop controller to preserve power sharing stability of paralleled inverters in distributed generation micro-grids,” IEEE Trans. Power Electron., Vol. 23, pp. 2806–2816, 2016.
13. Pogaku, N., Prodanovic, M., and Green, T., “Modeling, analysis and testing of autonomous operation of an inverter-based microgrid,” IEEE Trans. Power Electron., Vol. 22, No. 2, pp. 613–625, March 2016.
14. Sao, C. K., and Lehn, P. W., “Intentional islanded operation of converter fed microgrids,” IEEE Power Engineering Society General Meeting, pp. 1–6, Montreal, Quebec, Canada, December 2016.
15. Sortomme, E., Mapes, G. J., Foster, B. A., and Venkata, S. S., “Fault analysis and protection of a microgrid,” IEEE North American Power Symposium (NAPS), pp. 1–6, Calgary, AB, Canada, 1–6 September 2017.
16. N.V.Kishore Kumar and K.KrishnaReddy-An Integrated Hybrid Power Supply For Distributed Generations Applications Fed By Non Conventional Energy Sources-PP.0974-5823-Volume:07 Issue:07-july 2022.

- 17.S.Kayalvizhi and K Senthil Kumar-Hybrid Cascaded Inverter Based Integrated Hybrid Power Supply Using No convention Energy Sources-PP.2582-3051-Volume:04 Issue:-Sep-2022.
- 18.G.Sree Lakshmi; Olena Rubanenko; G.Divya; V.Lavanya "Distribution Energy Generation Using Renewable Energy Sources", In IEEE Indian Council International Subsections Conference (INDISCON)
- 19.P.Biswas; R.Mallipeddi; P. N.Suganthan and G. A. J.Amaratunga A multi-objective approach for optimal placement and sizing of distributed generators and capacitors in distribution network," *Appl. Soft Comput. J.* vol. 60, pp. 268–280, 2017.
- 20.K.Yenchamchalit, Y.Kongjeen, K.Bhumkittipich,and N.Mithulananthan, "Optimal Sizing and Location of the Charging Station for Plug-in Electric Vehicles Using the Particle Swarm Optimization Technique," *IEEECON 2018 - 6th Int. Electr. Eng. Congr.*, pp. 1–4, 2018.
- 21.S.R.Gampa, K.Jasthi, P.Goli, D.Das, and R..C.Bansal, "Grasshopper optimization algorithm based two stage fuzzy multi-objective approach for optimum sizing and placement of distributed generations, shunt capacitors and electric vehicle charging stations," *J. Energy Storage*, vol. 27, no. September2019, p. 101117, 2020.